Available online at www.sciencedirect.com

ScienceDirect

Procedia Materials Science 8 (2015) 934 – 943

Procedia Materials Science

www.elsevier.com/locate/procedia

International Congress of Science and Technology of Metallurgy and Materials, SAM - CONAMET 2013

Wear Resistance of Fe-based Nanostructured Hardfacing

Agustín Gualco[a]*, Cristian Marini[a], Hernán Svoboda[b,c], Estela Surian[a,d]

[a] *Research Secretariat, Faculty of Engineering, National University of Lomas de Zamora, Lomas de Zamora, Province of Buenos Aires, Argentina.*
[b] *Materials and Structures Laboratory, Faculty of Engineering, University of Buenos Aires, INTECIN, CONICET, Buenos Aires, Argentina.*
[c] *CONICET-Consejo Nacional de Investigaciones Científicas y Técnicas, City of Buenos Aires, Argentina.*
[d] *DEYTEMA, Regional Faculty of San Nicolás, National Technological University, San Nicolás, Province of Buenos Aires, Argentina.*

Abstract

The purpose of this work was to study the microstructural evolution and wear resistance of a nanostructured iron-based alloy deposited by FCAW process. Two samples with one and two layers were welded under Ar-20CO_2 shielding and heat input of 3.5 kJ/mm. Chemical composition was determined and microstructure was studied using both optical and scanning electron microscopy and X ray diffraction. Hardness, cristallite size, percentage of dilution and abrasive wear resistance were measured. The hardness of the deposit was found between 800 and 920 HV_2, depending on the number of layers as well as the chemical composition of the samples. The wear test results were discussed in relation to chemical composition, microstructure and hardness.

Selection and peer-review under responsibility of the scientific committee of SAM - CONAMET 2013

Keywords: hardfacing ; FCAW, nanomaterials; abrasive wear

1. Introduction

The technology of materials has experienced significant progress over the last years, especially in terms of surface coatings, with currently available specific coatings applicable to particular purposes and resistant to different types of demands. In this aspect, the systematic study of consumables and welding procedures applied to hard surfacing is of great interest for the optimization of the consumables design and for the assessment and tuning of

* Corresponding author. Tel.: 011-4282-7880; fax: 011-4282-7880.
E-mail address: agustingualco@yahoo.com.ar

Selection and peer-review under responsibility of the scientific committee of SAM - CONAMET 2013
doi:10.1016/j.mspro.2015.04.154

welding procedures. Within this context, heat input, shielding gas composition, pre-heating temperature and post-welding heat treatment are some of the most relevant variables of the welding procedure (Linnert, G, 1994).

Modern metal cored wires allow depositing layers providing a broad spectrum of almost optional chemical compositions e.g. iron based alloys and iron based alloys with liquid metal-like structures called nanostructure (Linnert, G, 1994; Merrick, S. et al., 1998; Heath, G., 2006).

These materials have a high hardness due to their extremely small crystallite size, about 30 to 50 nm. They can also form ultra-hard precipitates as niobium, boron or tungsten carbides which improve abrasive wear resistance. They are applied on new or worn working surfaces of machine parts or elements to provide specific properties as abrasive and adhesive wear resistance, erosion resistance, corrosion resistance, heat resistance and many of their combinations (Linnert, G, 1994). It is reported that 50-60% of machine elements are worn due to erosive and abrasive wear which has many forms including low stress, high stress, dry or wet abrasion (Linnert, G, 1994; Merrick et al., 1998; Klimpel et al., 2005).

Abrasion wear resistance of FCAW surfaced layers is a function of the microstructure which depends on different variables such as chemical composition, solification and cooling rate (Merrick, S. et al., 1998; Klimpel, A., 2006). In turn, the heat input, which depends on welding parameters (voltage, current intensity and welding velocity) and defines the thermal cycle, strongly influences the solidification structure of the deposited material; it also allows controlling the shape of fusion line, the bead penetration depth and the percentage of dilution, thus chemical composition of the deposit. Previous work (Evans, G., 1982; Gualco, A. et al., 2010; Francis, J., 1999) have shown that the variations of the heat input causes changes in both the chemical composition and the microstructure of the deposited metal and consequently variations in the final properties of the deposit. In nanostructured alloy deposits it was observed that dilution is the mayor factor influencing the structural characteristics of these materials, since the crystallite size of the matrix is primarily defined by the chemical composition (Weissmiiller, J., 1993). However there is scarce available information on systematic studies with this kind of consumables, particularly with Fe-based nanostructured hardfacing deposits, then it results particularly relevant to know how different heat inputs modify the chemical composition and other aspects of the deposited metal. The purpose of this work was to study the influence of the number of layers on the percentage of dilution, the microstructure, the crystallite size and the hardness of Fe based nanostructured deposits.

2. Experimental procedure

2.1. Welding consumable

The consumable studied was a 1.6 mm diameter flux-cored tubular wire, which generated a Fe based nanostructured deposit. It was welded using a power source for pulsed semi-automatic arc welding under Ar-20CO_2 mixture shielding with a gas flow of 18 L/min and using a stick out of 20 mm. All the weldments were performed using a Miggytrac automation system.

2.2. Welding pad for all-weld metal chemical composition determination.

In order to determine the all-weld-metal chemical composition, a coupon was welded according to Figure 1. The sequence was 3 layers of 4, 3 and 2 beads per layer. The welding parameters used were 300 A, 35 V and 5 mm/s of welding speed. The chemical composition was measured on the last weld bead.

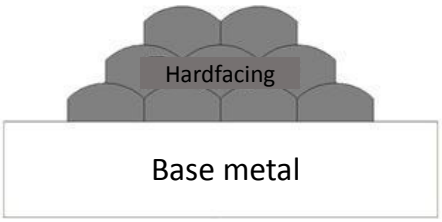

Fig. 1. Scheme of all weld metal coupon.

2.3. One and two layers coupons for the wear study (WS).

Two test coupons of 150 x 75 x 12.5 mm AISI 1010 carbon steel plate were surfaced by welding according to Figure 2. The welding parameters employed, chosen from previous works (Gualco, A. et al. 2012), can be seen in Table 1, as well as the sample identifications.

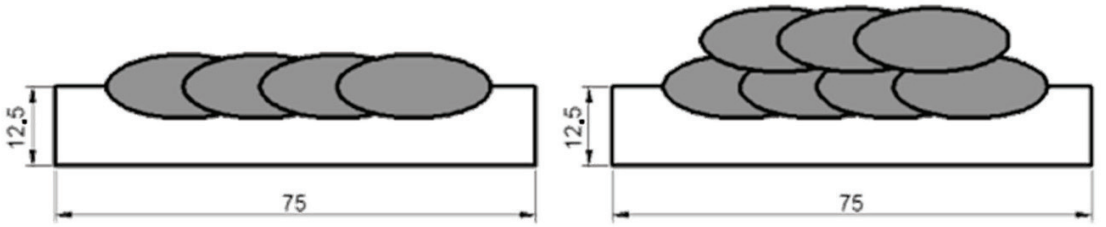

Fig. 2. Scheme of the coupons; units in mm.

Table 1. Welding parameters.

Identification	Layers	Volt (V)	Current (A)	Welding velocity (mm/s)	Heat input (kJ/mm)
A1	1	35	300	3	3.5
A2	2	35	300	3	3.5

After been welded, the samples were visually inspected to detect the presence of macroscopic surface defects.

2.4. Chemical and microstructural characterization in WS coupons

On cross sections of each welded specimens for wear studies, chemical composition was measured by energy dispersive spectrometry X-ray (EDS) and microstructure was characterized by optical microscopy (LM) and scanning electron microscopy (SEM).

X-ray diffraction (XRD) was performed on the surface of the coupons, in the hatched area of Figure 3. The equipment employed was a RIGAKU with Cu tube and K-α radiation. Profiles were performed from 35 ° to 95 ° with a speed of 1 degree per minute. The phases present were analyzed and crystallite size was determined using Scherrer's formula (Cullity, B. et al., 2001).

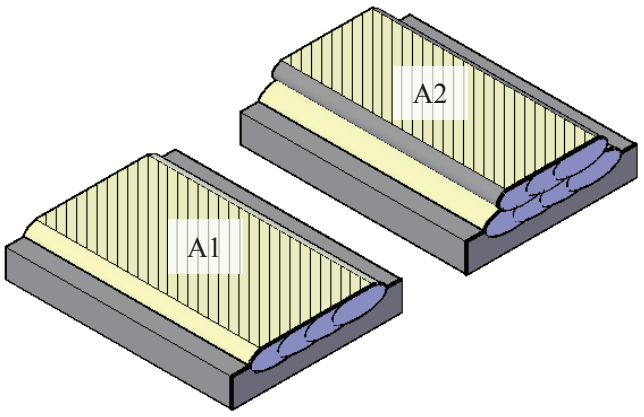

Fig. 3. Hatched area: place where X-ray diffraction was performed.

2.5. Dilution study in WS coupons.

Percentage of dilution was studied through both, the volume analysis and the chemical composition differences between the base metal and the beads.

2.6. Microindentation test and abrasive wear resistance in WS coupons.

On cross sections obtained from the WS, horizontal profile of hardness (HV_2) was performed at 1mm from the surface.

To determine the abrasive wear resistance three samples of each WS coupons were extracted. The abrasion tests were performed according to standard ASTM G65-04 "Standart Test Method for Measuring Abrasion Using the Dry Sand/Rubber Wheel Apparatus". The specimen was pressed onto the surface of rubber wheel rotating at 200 rpm, with a force of 130 N, while an abrasive is introduced between the wheel and the specimen at a constant flow rate of 320 g/min. The wear was evaluated by the weight loss of the sample.

3. Results and discussion

3.1. All weld metal chemical composition

Table 2 shows the results of chemical analysis obtained from all weld metal.

Table 2. All weld metal chemical composition (% weight).

C	Mn	Si	Cr	Nb	B	Fe
0.99	0.22	1.02	16.8	4.6	4.6	balance

The deposit showed a high concentration of alloying elements, within the system Fe-(Nb, Cr) - (C, B). The chemical composition complies with the rules for the formation of nanostructures which are: a difference in atomic radius greater than 12%, the system is multi-component with at least three alloying elements and the heat of mixing between the elements is negative (TeroMatec 395NOA, 2008; Gleiter, H., 2000; Inoe, A., 2010).

3.2. WS analysis

3.2.1. Visual inspection

In Figure 4 the surface appearance of the first layer is presented.

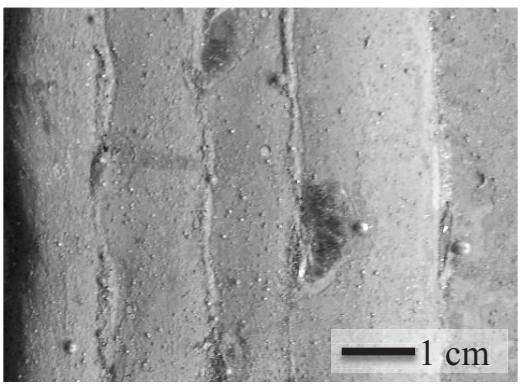

Fig. 4.Surface view of the welded beads.

It was observed that in the WS specimens the spatter levels and slag generation were low. In addition, the beads showed good surface finish.

3.2.2. Macrography and analysis of layers

Figure 5 shows the photomacrographs of different cross sections of the WS coupons. It can be seen that both the base metal and the deposit, showed absence of macroscopic defects such as pores and inclusions. In most of them cracks that were produced during cooling of the welded bead were found.

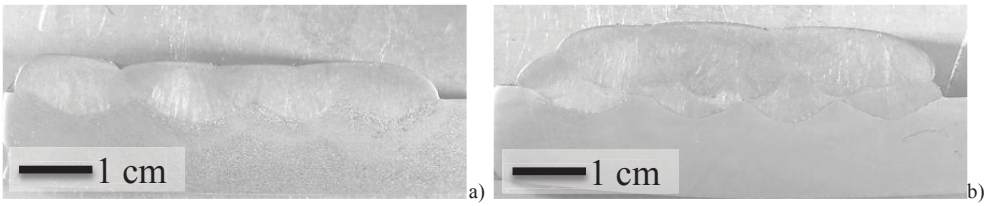

Fig. 5. Macrographs of the welded specimens, a) A1, b) A2.

Based on the geometries of the beads the volumetric dilution (Merrick, S. et al., 1998) of each sample was calculated using a software of image analysis. The first layer presented a dilution of 31% and the second 16%.

3.2.3. Microstructural characterization

Figure 6 shows XRD patterns obtained for the one and two layer WS coupons, A1 and A2.

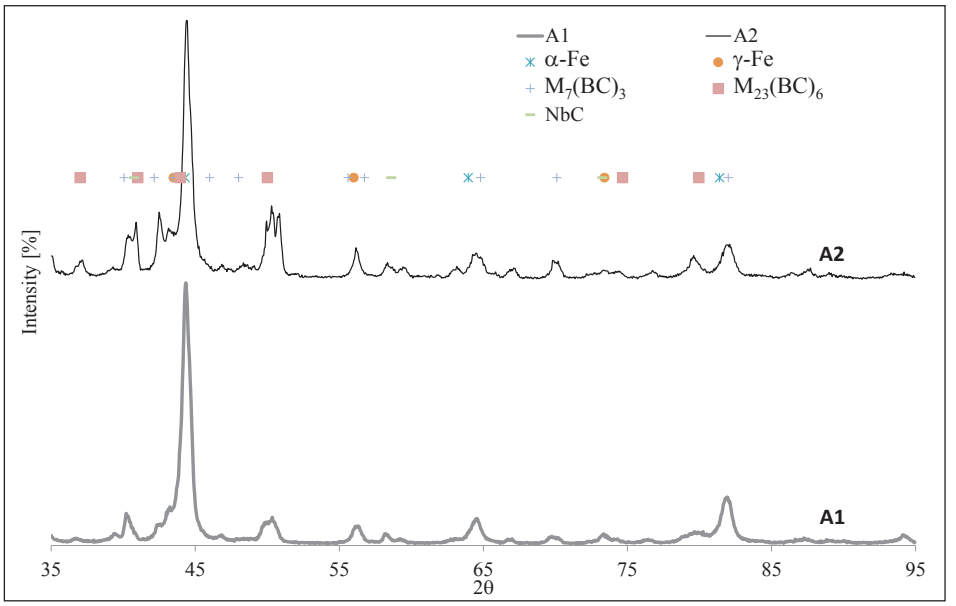

Fig. 6. XRD patterns for both conditions.

It can be seen that the microstructure consisted mainly of α-Fe; it was also detected a low fraction of γ-Fe and metallic carboborides ($M_7(BC)_3$, $M_{23}(BC)_6$) and niobium carbide (NbC). The crystallite size measured by using XRD pattern were 110 nm and 134 nm for A1 and A2, respectively. These variations could be related to the total

percentage of precipitates, which could affect the distribution of alloying elements (Branagan, D., 2006) and therefore the crystallite size of the nanocrystals

Table 3 shows the percentage of the phases present in each sample. These values were calculated using XRD patterns and a phase analysis software (Xpowder, 2004).

Table 3. Quantification of phases.

Specimen	α-Fe [%]	γ-Fe [%]	$M_{23}(BC)_6$ [%]	$M_7(BC)_3$ [%]	NbC [%]
A1	61	5	15	18	1
A2	46	6	20	26	2

Table 3 shows that the specimen welded with two layers presented an increase in the amount of precipitates. This could be related to lower dilution effect, producing a material rich in alloying elements, which would enhance the formation of carbides (Branagan, D., 2006; Gualco, A. et al., 2005).

Regarding the microscopic observation, in Figure 7, SEM images of the microstructures obtained for the different welding conditions are shown.

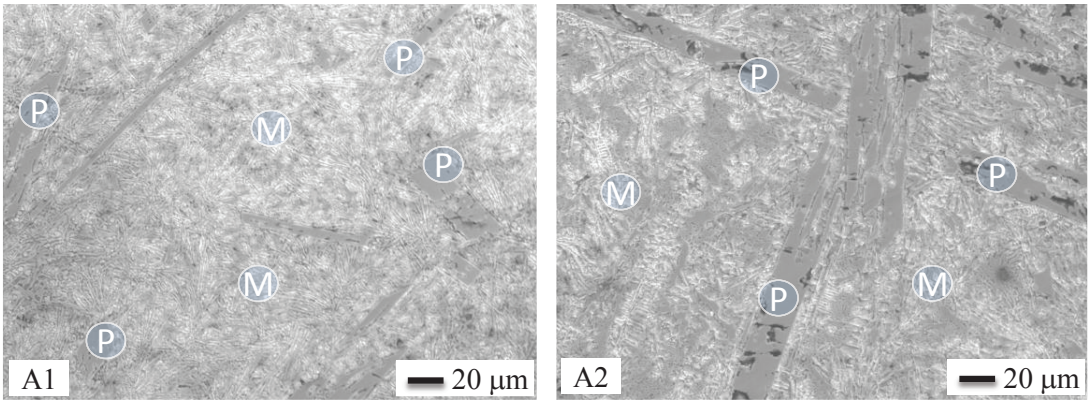

Fig. 7. SEM micrographs of the A1 and A2 samples.

It was observed that the matrix was formed by α-Fe (M) with carbides (P) of elongate shape $M_{23}(BC)_6$. The quantity of them are higher for the A2 specimen. Furthermore in matrix zone there was seen a laminar-globular structure, which is formed by α-Fe and $M_7(BC)_3$. Figure 8 shows a detail of this area.

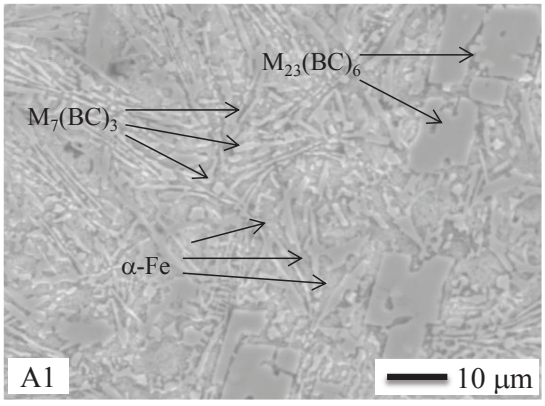

Fig. 8. Detail of the microstructure of the A1 specimen.

The quantity of alloying elements in the matrix was higher for A1 (12% Cr) than for A2 (9% Cr). This higher concentration of alloying elements in the matrix was consistent with the smaller amount of carbides presented in the sample A1. It was not found Nb in the matrix in any of the samples. This was associated with the formation of NbC carbides, as shown in Figure 9.

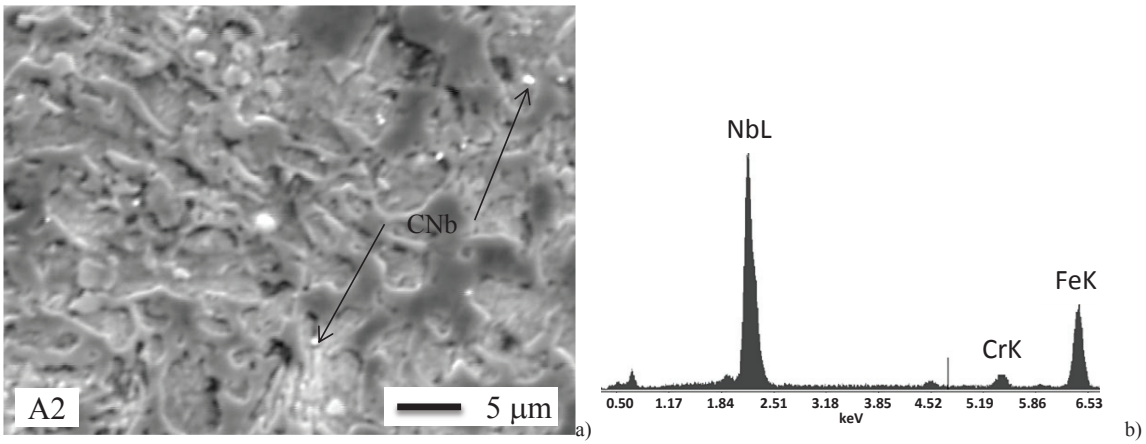

Fig. 9. a) Carbides of Niobium for A2 and b) EDS.

3.2.4. Hardness

Figure 10 shows the results of hardness measured at 1 mm from the top surface of the beads.

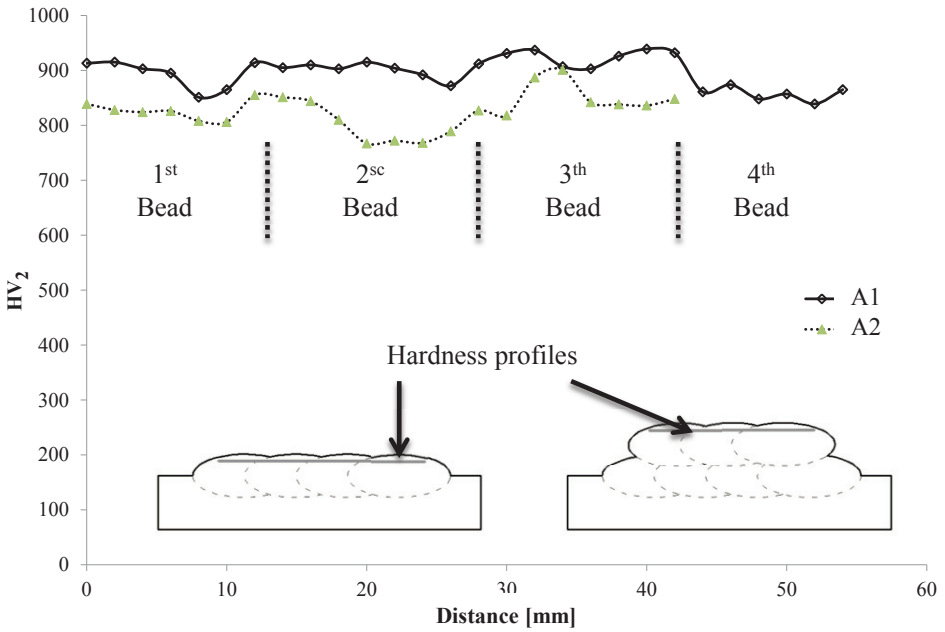

Fig. 10. Hardness profiles measured at 1 mm from the surface of each layer.

It can be observed that the values varied between 800 and 920 HV, being consistent with what was expected for this material (Branagan, D. et al., 2006). The variatons presented by each specimen could be related to the effects of

dilution and interpass tempering (Gualco, A. et al, 2005). Furthermore, the specimen with one layer showed higher hardness which could be associated with both smaller size and larger saturation of the crystallite, as observed previously (Fougere, R. et al., 1993; Weissmiiller, J., 1994; Morris, D., 2010; Inoe, A., 2005).

3.2.5. Wear study

Table 4 shows the results of weight loss as an average of three measurements per condition.

Table 4. Values of weight loss for the A1 and A2 samples.

	Specimen	Weight before test [g]	Weight after test [g]	Weight loss [g]	Average weight loss [g]
A1	1	101.1998	101.0618	0.1380	0.1457
	2	98.9877	98.8409	0.1468	
	3	102.7756	102.6234	0.1522	
A2	1	107.2602	107.1499	0.1103	0.1053
	2	105.4873	105.3890	0.0983	
	3	106.8541	106.7469	0.1072	

For each condition, the values varied around 10%, consistent with what was expected for this type of test. The specimens welded with two layers showed higher wear resistance than the one with one layer, about of 38%. This could be associated with the presence of higher amount of hard carbides in the deposit, which improved abrasive wear resistance (Inoe, A., 2005; Kato, K., 1997; Zum Gah, K., 1998).

Figure 11 shows a SEM image of the worn surface. The analyzed area belongs to the center of the wear surface. Abrasion lines were detected with the same direction of the sliding, produced by the sand scratched. The presence of carbides, which were confirmed by EDS were also observed. The thickness of the grooves was between 1 and 20 μm.

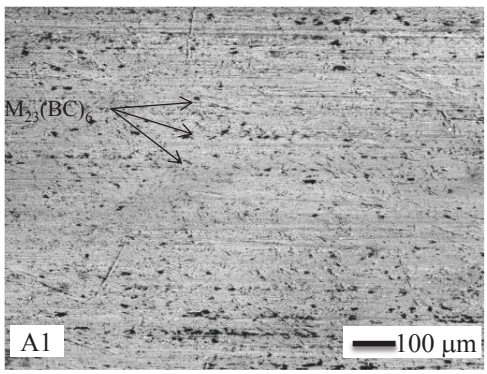

Fig. 11. SEM image of the A1 worn surface.

Figure 12 shows two longitudinal sections of the specimens tested.

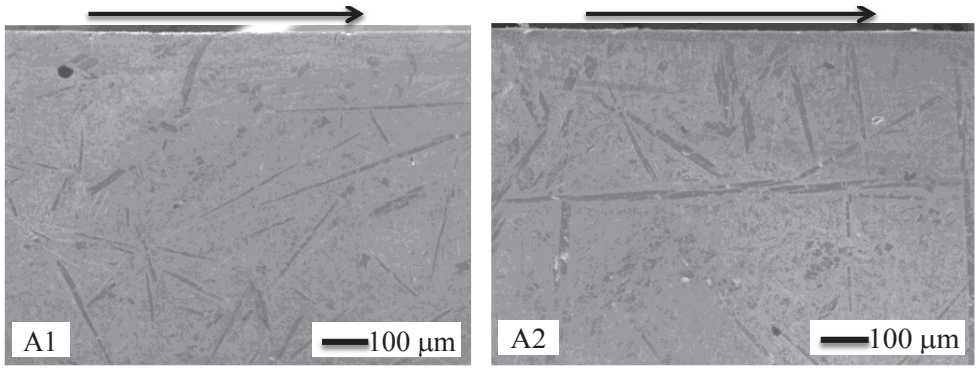

Fig. 12. Longitudinal section of A1 and A2 worn specimens.

In SEM pictures, Figure 12, a larger presence of hard carbides in the A2 specimen could be detected. This is consistent with what was found in the diffraction patterns. These elongated shape carbides of a few hundred microns length, improved the wear resistance.

4. Conclusions

Evaluating the effect of the number of layers on the microstructural evolution and wear resistance of a nanostructured iron-based alloy deposited by FCAW process, it was concluded that:

- All welded specimens showed good surface finish, low levels of spatter and slag. Most of them showed cracks during cooling
- The microstructure was comprised of primarily α-Fe; it was also detected a low fraction γ-Fe and metallic carboboruros ($M_7(BC)_3$, $M_{23}(BC)_6$) and niobium carbide (NbC). The crystallite size measured on XRD pattern was 110 nm and 134 nm for A1 to A2 specimens respectively. This increase in crystallite size might be caused by the decrease of alloy content.
- The hardness decreased with the second layer from 920 to 800 HV, for extreme values. This decrease of hardness could be associated with higher crystallite size.
- The wear resistance was higher for the specimen welded with two layers. This could be associated with the increased presence of ultra-hard carbides.

Acknowledgements

The authors wish to express their gratitude to EUTECTIC-CONARCO, Argentina for the donation of the consumable, to EUTECTIC-USA for performing chemical analysis, to AIR LIQUIDE Argentina for donating the welding gases, to the Scanning Electron Microscopy Laboratory of INTI-Mechanics, Argentina, for facilities for SEM analysis and to APUEMFI, Argentina for financial support.

References

Linnert, G, 1994. Welding metallurgy carbon and alloy steels, 4 ed. AWS: Miami, Florida, p. 474.

Merrick, S., Kotecki, D., Wu, J., 1998. Materials and applications - Part 2, Welding Handbook, American Welding Society.

Heath, G., 2006. Nanotechnology and Welding – Actual and possible future applications; Proceedings of the CASTOLIN-EUTECTIC SEMINAR, Brussels: Belgium, 2006, p. 25-35.

Klimpel, A., 2006. Robotized GMA surfacing of cermet al deposits, Journal of Achievements in Materials and Manufacturing Engineering; Vol. 18 (2006), p.395-398.

Klimpel, A., Janicki, D., 2005. A study of worn wear plates of fan blades of steel mill fumes suction system; Proceedings of the 13th Scientific International Conference, Achievements in Mechanical and Materials Engineering AMME'2005, Polonia: Gliwice. p. 307-310.

Evans, G., 1982. The effect of heat input on the microstructure and properties of C-Mn all-weld-metal deposits. Welding Journal, Vol. 61, p. 125s-132s.

Gualco, A., Svoboda, H., Surian, E., De Vedia, L., 2010. Effect of welding procedure on wear behaviour of a modified martensitic tool steel hardfacing deposits; Materials & Design, Vol. 31, p. 4165-4173.

Francis, J., 1999. Principles for open-arc weld deposition of high-chromium white iron surface layers; Adelaide Editor.

Weissmiiller, J., 1993. Alloy effects in nanostructures; Nanostructured Materials, Vol. 3, p. 261-272.

Gualco, A., Svoboda, H., Surian, E., 2012. Efecto del calor aportado en recargues nanoestructurados base hierro; XXXVIII CONSOLDA – Congresso Nacional de Soldagem,.

Cullity, B.,Stock, S., 2001. Elements of x-ray diffraction; 3 ed. Prentice Hall, P.520.

TeroMatec 395NOA, 2008. Datasheet of Eutectic Castolin-ESAB, USA.

Gleiter, H., 2000. Nanostructured materials: basic concepts and microstructure; Acta Materialia, Vol. 48, n.1, p. 1-29.

Inoe, A., 2010. Amorphous and nanocrystalline materials: Preparation, properties, and applications; Springer, p.206.

Branagan, D., Marshall, M, Meacham, B., 2006. High toughness high hardness iron based PTAW weld materials; Materials Science and Engineering A 428, p. 116–123.

Xpowder, 2004. Software de análisis de espectros de difracción.

Gualco, A., Svoboda, G., Surian, E., Ramini, M., De Vedia, L., 2005. Estudio de dilución en depósitos de soldadura para recargues duros; SAM/CONAMET, Mar del Plata.

Fougere, R., Weertman, J., Siegel, R., 1993. “On the hardening and softening of nanocrystalline materials”; Nanostructured Materials Journal, Vol. 3, n.1-6, p. 379-384.

Weissmiiller, J., 1994. Some basic notions on nanostructured solids; Materials Science and Engineering, A Vol.179-180, p. 102-107.

Morris, D., 2010. “The origins of strengthening in nanostructured metals and alloys”; Revista de metalurgia, Vol.46, n.2, p. 173-186.

Inoe, A., 2005. Bulk glassy and nonequilibrium crystalline alloys by stabilization of supercooled liquid: fabrication, functional properties and applications (Part1); Proc. Japan Acad., Vol. 81, Ser.

Kato, K., 1997. Abrasive wear of metals. Tribolgy International; Vol 30, 5, p. 333-338.

Zum Gah, K., 1998. Wear by hard particles; Tribolgy International, Vol 31, 10, p. 587-596.